Hydrophobic Core of the Steroidogenic Acute Regulatory Protein for Cholesterol Transport[†]

Himangshu S. Bose,*[,‡] Randy M. Whittal,[§] Mahuya Bose,[‡,||] and Dilip Debnath[‡]

Department of Biomedical Sciences, Mercer University School of Medicine and Memorial Health University Medical Center, Savannah, Georgia 31404, and Department of Chemistry, University of Alberta, Edmonton, Alberta T6G 2G2, Canada

Received August 11, 2008; Revised Manuscript Received December 22, 2008

ABSTRACT: The steroidogenic acute regulatory protein (StAR), the first family member of START (StAR-related lipid transport) proteins, plays an essential role by facilitating the movement of cholesterol from the outer to inner mitochondrial membrane. Wild-type and mutant StAR binds cholesterol with similar intensity, but only wild-type StAR can transport it to mitochondria. Here, we report that the hydrophobic core is crucial for biological activity of proteins with START domains. Wild-type StAR increased steroidogenic activity by 7−9-fold compared to mutant R182L StAR, but both of them showed similar near-UV CD spectra. The fluorescence maximum of wild-type StAR is red shifted in comparison to mutant StAR under identical urea concentration. TFE increased the α-helical contribution of wild-type StAR more than the mutant protein. Acrylamide quenching for the wild-type protein ($K_{SV} = 12.0 \pm 0.2-11.2 \pm 0.5\ M^{-1}$) exceeded that of the mutant protein ($K_{SV} = 4 \pm 0.2\ M^{-1}$). Consistent with these findings, the hydrophobic probe ANS bound wild-type StAR ($K_{app} = 8.1 \times 10^5\ M^{-1}$) to a greater degree than mutant StAR ($K_{app} = 3.75 \times 10^5\ M^{-1}$). Partial proteolysis examined by mass spectrometry suggests that only wild-type StAR has a protease-sensitive C-terminus, but not the mutant. Stopped-flow CD revealed that the time of unfolding of mutant StAR was 0.017 s. In contrast, the wild-type StAR protein is unfolded in 16.3 s. In summary, these results demonstrate that wild-type StAR adopts a very flexible form due to the accommodation of more water molecules, while mutant StAR is generated by an alternate folding pathway making it inactive.

Protein misfolding is critical to both normal and pathologic conditions. To become functional, newly synthesized protein chains must be folded, via a nonspontaneous process, into unique three-dimensional structures. Although the native fold is encoded in the amino acid sequence (*1*), proteins with diverse sequences may fold very similarly, giving rise to comparable structures and properties. Protein folding and activity are directly linked. Proteins may acquire activity in an unfolded state, in intermediate states, or, more generally, in the completely folded form (*2*). The folding reactions of small proteins and protein domains reflect the conformational diffusion of the unfolded polypeptide across an energy barrier separating the native structure and a manifold of unfolded structures (*3, 4*). The folding of these proteins is limited only by the intrinsic features of the energy surface, which are governed by chain topology and amino acid sequence (*5*). In large proteins, the folding reactions have complex kinetics, indicative of a significant role for alternative conformational states.

The steroidogenic acute regulatory protein (StAR)[1] is a 285 amino acid phosphoprotein with a mitochondrial targeting sequence (*6*). On hormonal stimulation StAR is synthesized in the cytoplasm of adrenal and gonadal cells and acts exclusively at the outer mitochondrial membrane (OMM) (*7*) for the movement of cholesterol from the outer to the inner mitochondrial membrane (IMM). After cholesterol enters into the mitochondria, the side chain cleavage enzyme at the mitochondrial matrix catalyzes it into pregnenolone. Pregnenolone is the first steroid in the tissue, and thus it is the precursor of all steroid synthesis. Expression of StAR is essential for the survival of all species. Mutant StAR cannot transport cholesterol, resulting in an inborn disorder in metabolism, in which fetuses die shortly after birth due to a salt-losing crisis (*8*). After genetic analysis of more than two dozen lipoid CAH patients from six continents, we find two common mutations. Replacement of arginine by leucine at position 182 of StAR (R182L) is common among the Arab population, and replacement of glutamine by a stop codon at position 258 (Q258X) is common in the Japanese and Korean populations (*8*).

[†] This work was supported by a grant from the National Institutes of Health (RO1 HD057876), March of Dimes, American Heart Association, and Pfizer, Inc.

* To whom correspondence should be addressed. Tel: 912-350-1710. Fax: 912-350-1765. E-mail: bose_hs@mercer.edu and bosehi1@memorialhealth.com.

[‡] Mercer University School of Medicine and Memorial Health University Medical Center.

[§] University of Alberta.

[||] Present address: Center for Health Regeneration Biotechnology, 13702 Innovation Dr., Alachua, FL 32615.

[1] Abbreviations: StAR, steroidogenic acute regulatory protein; START, StAR-related lipid transport domain; Preg, pregnenolone; MS, mass spectrometry; Mito, mitochondria; OMM, outer mitochondrial membrane; IMM, inner mitochondrial membrane; Chol, cholesterol; ANS, 1-anilinonaphthalene-8-sulfonic acid; TFE, 2,2,2-trifluoroethanol; 22-*R*, 22(*R*)-hydroxycholesterol; NATA, *N*-acetyl-L-tryptophanamide; VDAC, voltage-dependent anion channel.

10.1021/bi801514e CCC: $40.75
Published on Web 01/26/2009

StAR entry into mitochondria is not necessary for activity, as deletion of the first 62 amino acids encoding the mitochondrial targeting sequence (N-62 StAR) does not alter the steroidogenic activity of the protein in COS-1 cells (*9*) or incubation of biosynthetic N-62 StAR in the presence of isolated mitochondria from steroidogenic cells. Transfection of full-length mutant and wild-type StAR, followed by Western blotting, shows that the proteins are processed similarly and both reach the mitochondrial matrix (*8*). The 62 amino acid truncated StAR (N-62 StAR) or full-length StAR exhibit maximal activity when permanently affixed to the OMM (*10*). Under similar conditions, the 62 amino acid truncated mutant R182L StAR was inactive. Thus the truncated form (N-62 StAR) is similar to full-length StAR while mutant R182L N-62 StAR is similar to full-length mutant R182L StAR. Thus, herein we refer to N-62 StAR as wild-type StAR and mutant R182L N-62 StAR as mutant StAR.

The C-terminal 210 residues of StAR are conserved across species and serve as a versatile binding surface for lipids in many distinct processes in different tissues including fostering of cholesterol (*11, 12*). These are called START for StAR-related lipid transport domain proteins. The first StAR family member was StARD1, and the rest of the family members are denoted numerically (i.e., StARD3, StARD4, etc.). There are several START domain-containing proteins that have been identified in species ranging from plants (*Arabidosis*, birch trees) to worms (*Caenorhabditis elegans*) to mammals (*13, 14*).

Functional characterization of START-domain proteins has been performed by cotransfecting them into nonsteroidogenic COS-1 cells with F2 vector (*15*) and measuring pregnenolone synthesis. Such studies have found that StARD3 has 40−50% of the activity of truncated N-62 StAR or full-length StAR (*16*), while StARD4 has less than 30% of the activity of StAR (*17*). In contrast, in COS-1 transfected cells StARD5 showed the same activity as the StAR mutant (R182L) (*17*). The StAR mutant that causes lipoid CAH contains a change in one amino acid, and it is completely inactive. Surprisingly, StARD3 has 37% amino acid identity to StAR, and it has 40−50% StAR-like activity, so sequence variation is not the sole reason for StAR inactivity. The crystal structures of START-domain proteins, including StARD3 (*18*) and StARD4 (*19*), along with the cocrystal structure of StARD2 (*20*), show similar three-dimensional structures. Baker et al. recently reported a model StAR structure in the presence of cholesterol (*21*). The molecular dynamics studies of StAR in the presence of cholesterol (*22*) also supported the model StAR structure originally proposed by Tsujishita and Hurley (*18*). Mutant StAR can bind to cholesterol with an affinity similar to that of wild-type StAR (*22, 23*), but only wild-type StAR can transfer cholesterol to mitochondria (*24, 25*). Thus, there is likely specificity in the folding of wild-type StAR that helps in the discharge of cholesterol. This was further evidenced using fluorescence resonance energy transfer, which demonstrated that wild-type StAR can transfer cholesterol five times faster to synthetic membranes than can mutant StAR (*26*). Using cellular techniques we have found that wild-type StAR docks at the OMM-associated VDAC1 required for its import and activity (*10*). Thus, there appears to be a specific mechanism regulating the biological activity of StAR proteins or perhaps cholesterol is imported with the help of StAR and peripheral benzodiazapine receptor (PBR, also called TSPO) (*24*).

Our recent results (*28*) provide strong evidence that environmental conditions are extremely important for StAR activity. For example, incubation of mitochondria with nicotine did not have any effect with the mitochondrion itself but has a significant effect on the folding of StAR, which finally affects mitochondrial import and activity (*29*). This is specific for StAR but not of other proteins; when ^{35}S-labeled StAR was incubated with isolated mitochondria from the adrenals or steroidogenic cells, its import efficiency decreased. Spectroscopic studies showed very similar far-UV CD spectra of the wild-type StAR and mutant StAR proteins (*27*). Similarly, limited proteolysis with trypsin of three START (StARD1, StARD3, and StARD6) proteins having StAR-like activity yielded similarly sized fragments (*16, 30*), suggesting that the overall folding of the active proteins was the same. We have observed that the unfolding rate is dependent on the environment. Thus, the environmental conditions are extremely important for proper folding of StAR where wild-type StAR remained more flexible, due to its different folding pathways, than mutant StAR. This could be attributable to the different rates of refolding associated with the mutant proteins or because of its strong hydrophobic clusters formed by branched aliphatic side chain amino acids making the mutant very compact and rigid (*31*). Therefore, the internal organization of StAR is very important for its activity. Any change in the organization of the internal folding of the protein affects its activity.

We have observed that slower unfolding increases StAR activity (*30, 32*). Here, we show that the hydrophobic core of the mutant is less accessible than the active StAR proteins and that preservation of flexibility of StAR is essential for activity.

MATERIALS AND METHODS

Protein Purification. Transformed *Escherichia coli* were grown with ampicillin and kanamycin at 37 °C to an optical density of 0.5, then transferred to 15 °C, induced with 0.4−1 mM IPTG, and allowed to grow for an additional 12 h. Bacterial pellets containing the expressed constructs were resuspended in lysis buffer (50 mM NaH_2PO_4, 300 mM NaCl, and 10 mM imidazole, pH 8.0) and sonicated on ice with 10 s pulses and 30 s rests for 10 min. The soluble fraction was separated by centrifuging at 15000*g* for 30 min and then passed through a Ni-NTA column washed first with lysis buffer and then with 50 mM NaH_2PO_4, 300 mM NaCl, and 25 mM imidazole, pH 8.0. The column was then eluted with 250 mM imidazole, pH 7.5. The eluates were dialyzed against 20 mM NaH_2PO_4 and 50 mM NaCl, pH 7.4, then the proteins were purified through a gel-filtration column connected to a FPLC, and the concentrations of the unfolded proteins were determined with guanidine hydrochloride to avoid errors in extinction coefficients (*33*). Aspecific near-UV (250−360 nm) measurements were made using a 1.0 cm quartz cuvette at 3 mg protein/mL. Multiple scans were averaged to improve the signal-to-noise ratio. Appropriate buffer baselines were obtained under the same experimental conditions and were subtracted from the sample spectra. Data are shown as mean residue ellipticity $[\Theta]_r$.

Biological Activity. To determine bioactivity, we added biosynthetic wild-type StAR, StARD6, and mutant StAR protein to 20 μg of pig adrenal mitochondria in a final volume of 100 μL of bioassay buffer (*7*) (125 mM sucrose, 123 mM KCl, 5 mM $MgCl_2$, 10 mM NaH_2PO_4, 10 mM isocitrate, 25 mM HEPES, 0.1 mM ATP, and 10 μg/mL cholesterol, pH 7.4). The mixture was then incubated for 1 h at 37 °C and centrifuged at 10000*g* for 10 min, and pregnenolone synthesis was measured from the supernatant by radioimmunoassay (RIA) following appropriate dilutions.

Circular Dichroism. Far-UV (195−250 nm) circular dichroism (CD) measurements were carried out in an Aviv-215 spectropolarimeter at 20 °C with a 1.0 mm path length, rectangular cuvette containing 175 μg/mL (1.52×10^{-6} M) protein in 10 mM Tris-HCl, pH 7.5. Near-UV CD (aromatic CD) spectra were recorded from 250 to 360 nm, using a 1.0 cm cuvette at a protein concentration of 3.0 mg/mL. Spectra shown are averages of three consecutive scans that were performed at a scan speed of 20 nm/min, corrected by subtracting corresponding blanks, and subjected to noise reduction. Results are presented as mean residue molar ellipticity (Θ): $[\Theta]_r = \theta_{obs}/(10nlc)$, where θ_{obs} is the measured ellipticity in millidegrees, n the number of residues in the protein, l the path length of the cell expressed in cm, and c the molar concentration of protein. 2,2,2-Trifluoroethanol (TFE) was purchased from Sigma/Aldrich and was used without purification as volume percent (% v/v). The relative amounts of the three different types of secondary structure (i.e., α-helix, β-sheet, and random coil and turn) were calculated from far-UV CD spectra using CdPro software available online.

Western Blot Analysis. Affinity-purified recombinant N-62 StAR protein (100 ng) was separated on a 15% SDS−polyacrylamide gel and transferred to a polyvinylidine difluoride (PVDF) membrane (Millipore). This was blocked with 3% nonfat dry milk for 45 min, probed overnight with the antihuman N-62 StAR antiserum, and incubated with peroxide-conjugated goat anti-rabbit IgG (Pierce). Signals were developed with chemiluminescent reagent (Pierce).

Fluorescence Spectroscopy. Fluorescence spectra of different proteins were recorded in a Shimadzu spectrofluorometer (Shimadzu, model RF-5301PC) equipped with a variable emission and excitation band-pass. All of the fluorescence experiments were carried out at room temperature and at pH 7.5 using appropriate buffer constituents. Fluorescence quenching experiments were performed by the successive addition of 2 μL aliquots of 2 M acrylamide to the protein solution and by monitoring the change in Trp emission intensity at 340 nm. To correct for acrylamide absorption (295 nm), the measured intensity was multiplied by the antilog of OD/2, where OD is the optical density at 295 nm and 0.5 cm is the effective path length of the cell. The Stern−Volmer quenching constant (K_{SV}) was calculated as the slope of the linear region of the F_0/F_{corr} vs [Q] plots, where F_0 and F_{corr} are the corrected fluorescence intensities in the absence and presence of different concentrations of quencher molecule, respectively (*34, 35*).

Cholesterol Binding. Purified proteins in phosphate buffer were incubated with varying concentrations of NBD-cholesterol (Molecular Probes/Invitrogen) for 15 min at 37 °C, and fluorescence emission maxima were measured on a Shimadzu fluorescence spectrophotometer (Shimadzu, model 5301 PC) as described. The NBD-cholesterol was excited at 460 nm, and the emission intensity was recorded at 534 nm. The relative fluorescence intensity was measured following the procedure as described (*36, 37*). The collected data points were processed using Kaleidagraph or Microcal Origin (Origin Laboratory, MA).

Measurement of ANS−StAR Binding. Steady-state fluorescence experiments were performed using a Shimadzu (Shimadzu, model RF-5301PC) spectrofluorometer using a 10 mm path length quartz cuvette. Fluorescence spectra for 1-anilinonaphthalene-8-sulfonic acid (ANS) were recorded at an excitation of 357 nm with 5 nm band-pass slits for both excitation and emission channels. All experimental values were corrected for those obtained for buffer (10 mM Tris-HCl, pH 7.5) and free ANS run under identical conditions. The sample temperature was maintained at 25 °C for all experiments unless otherwise indicated. Stock solutions of 237.5 μM ANS in DMSO were diluted into water, and the concentration was determined using a molar absorption coefficient (ε) of 4990 M^{-1} cm^{-1} (*38*). Protein-ANS dissociation constants were determined by nonlinear curve fitting of the binding isotherm based on the following equilibrium: L + P → L−P, where L and P are ANS and protein, respectively. ANS binding experiments were performed using 5 μM protein, to which increasing amounts of ANS were added, and the emission intensity was measured at 470 nm to monitor protein-bound ANS in 14 different data points. The data points obtained from fluorometric titrations were analyzed by fitting to eqs 1 and 2. A total of 14 data points were recorded with a fixed increase in ANS concentration 1 μM maintaining protein concentrations unchanged. The dissociation constants of ANS binding to StAR (K_d) were determined by nonlinear curve fitting analysis using eq 2 (*38*). All of the experimental points for the binding isotherm were fitted by least-squares analysis using the Microcal Origin software package (Version 5.0; Microcal Software Inc., Northampton, MA). The binding stoichiometries of the ANS−protein complex were estimated from the intercept of two straight lines of the nonlinear fitted plot of $\Delta F/\Delta F_{max}$ against the mole fraction of ANS.

$$K_d = [(C_0 - \Delta F/\Delta F_{max})C_0][(C_p - \Delta F/\Delta F_{max})C_0]/(\Delta F/\Delta F_{max})C_0 \quad (1)$$

$$C_0(\Delta F/\Delta F_{max})2 - (C_0 - C_p + K_d)(\Delta F/\Delta F_{max}) + C_p = 0 \quad (2)$$

In both equations, ΔF is the change in fluorescence emission intensity at 470 nm ($\lambda_{ex} = 360$ nm) for each point on the titration curve, and ΔF_{max} is the change in fluorescence emission intensity when the protein is completely bound to ANS. C_p is the concentration of the ANS, and C_0 is the initial concentration of protein. The double reciprocal plot was used to determine ΔF_{max} following eq 3 and determined the apparent binding constant (K_{app}) (*39*).

$$1/\Delta F = (1/\Delta F_{max}) + 1/[K_{app}\Delta F_{max}(C_0 - C_p)] \quad (3)$$

The linear double reciprocal plot of $1/\Delta F$ against $1/(C_p - C_0)$ is extrapolated to the ordinate to obtain the value of ΔF_{max} from the intercept. The apparent binding constant, K_{app}, is the inverse of the dissociation constant (K_d). The approach is based on the change in emission intensity of ANS proportional to the concentration of the protein. C_p and C_0

represent protein (5 μM) and ANS concentration. Thus, the apparent binding rates reflect the ANS effect at the molten globule core as described from the changes with the incremental addition of ANS.

Proteolytic Digestion and Mass Spectrometry. Limited proteolytic digestion experiments of wild-type and mutant StAR were performed at room temperature using sequencing grade trypsin (Promega). For the proteolytic digestions, 5 μg of protein was incubated with 10 units of trypsin for varying periods of time. The reactions were terminated with the addition of an equal volume of 2 × SDS sample buffer containing 2 mM PMSF and immediately transferred to a boiling water bath. Following electrophoresis in a 22% SDS−PAGE, the samples were stained with Coomassie brilliant blue or silver nitrate. The visualized protected bands were excised, destained, reduced with DTT (Roche), alkylated with iodoacetamide (Sigma), and digested with trypsin (Promega sequencing grade modified) overnight (*40*) at 37 °C. The extracted peptides were analyzed via LC MS/MS on a nanoAcquity UPLC (Waters, MA) coupled with a Q-ToF-Premier mass spectrometer (Micromass, U.K./Waters, MA). Trypsin-digested peptide fragments were separated using a linear water/acetonitrile gradient (0.1% formic acid) on a nanoAcquity column (3 μm Atlantis dC18, 100 Å pore size, 75 μm i.d. × 15 cm) (Waters, MA), with an in-line Symmetry column (5 μm C18, 180 μm i.d. × 20 mm) (Waters, MA) as a loading/desalting column. Protein identification using the generated MS/MS spectra was performed by searching the NCBI nonredundant database using Mascot MS/MS Ion Search at www.matrixscience.com (Matrix Science, U.K.) with consideration for the carbamidomethylation of cysteine and the oxidation of methionine.

Stopped Flow. Protein unfolding kinetics were measured in an Aviv spectropolarimeter (Aviv-400) interfaced with a SF3 stopped-flow module (Biologic, France). To monitor the circular dichroic signal through stopped flow, we replaced the regular circular dichroic panel with a stopped-flow cell holder equipped with a water jacket and nitrogen flow line. An additional photomultiplier equipped with a filter holder was placed at a right angle to the light path to monitor fluorescence. Both cell and syringes were regulated at 25 °C by the use of an external water bath. The protein concentration in the syringe was 3 mg/mL, and the final concentration in the cell was 0.6 mg/mL. Aliquots of 36 μL of protein solution and 144 μL of 10 M urea, pH 7.5, were passed through a mixer, and the CD signals were measured. As the 10 M urea solution was very viscous, a "Delta" mixer was used, and syringes were operated at 3 mL/s. As a result, the dead time was relatively long, at about 9.7 ms. The unfolding rate was measured by monitoring the CD signal at 222 nm.

Each stopped-flow experiment was divided into four segments. In the first segment, 40 data points were acquired to monitor the signal of aged solution. Next, the solution was mixed for 60 ms. In the third segment, 100 data points were acquired during a period of 100 ms to monitor the fast kinetics, and 200 data points were acquired during a longer period of 2 s to assess the slow kinetics. To increase the signal-to-noise ratio, ten experiments were averaged and fitted to the following two-exponential decay equation (*41*): $I = \exp(-k_1 t) + \exp(-k_2 t) + I_0$, where I is fluorescence intensity at any time and k_1 and k_2 represent the rate constant for fast and slow unfolding, respectively. I_0 denotes the fluorescence at time zero. Each data point represents the mean of three to five individual experiments ± SD.

Protein Unfolding. To determine the stability of the protein, we measured the free energy of unfolding using urea, a commonly used nonionic chaotrope. Wild-type and mutant StAR (10 μg) were incubated with varying urea concentrations (0−8 M) for 12 h in a final volume of 300 μL. Fluorescence emission maxima (or intensity at 320 nm) were recorded, and the plot of intensity of emission maxima was measured as a function of urea concentration (*42*).

RESULTS

In Vitro Bioactivity. To study the cause of the inability of mutant StAR to transport cholesterol, we first purified milligram quantities of soluble protein from bacterial cytosol (Figure 1A), characterized it spectroscopically, and determined its activity. The purity of each preparation was confirmed spectroscopically. The chromatographic purification elution profile of all the proteins remained identical to one another (*27, 43*). Western blotting with N-62 StAR antiserum recognized all the fractions of wild-type StAR (Figure 1B). As a reminder, herein we refer to truncated N-62 StAR as "wild-type StAR" and truncated mutant R182L N-62 StAR as "mutant StAR".

To determine that these proteins were folded properly, we first determined pregnenolone synthesis capacity of the major purified fragments of all the proteins after incubating with pig adrenal mitochondria. We incubated StARD6 with the isolated mitochondria pig adrenals, and it was found to be equally active as wild-type StAR, and thus StARD6 was an additional control (*32*). Wild-type StAR or StARD6 synthesized 560 ng/mL pregnenolone, but mutant StAR protein showed pregnenolone synthesis activity similar to the level of buffer control or when the mitochondria were denatured by heat inactivation (Figure 1C).

To begin to understand the secondary structure of these proteins, we recorded the circular dichroism spectrum of wild-type and mutant StAR. Circular dichroism measures the absorption of circularly polarized light passing through a protein solution and generates a spectrum dependent on the chirality of the protein. Wavelengths in the far-UV CD region (185−250 nm) can identify changes in protein backbone structure (secondary structure), and those in the near-UV CD region (250−360 nm) identify hydrogen bonds formed by aromatic side chains (*44*). Far-UV CD spectra are good for characterizing α-helices with minima at 208 and 222 nm, β-sheets at 218 nm, and coils at or below 204 nm (*44*). In the near-UV CD (also called aromatic CD), positive and negative features in this region are most often associated with orientation and environment of the aromatic amino acid side chains, suggesting that the protein is likely folded (*44*). Our results revealed that spectra of wild-type StAR and mutant StAR were almost superimposable, suggesting that the secondary structure of both proteins was similar (Figure 1D, far-UV). Similarly, the near-UV CD spectra of wild-type and mutant StAR suggest their folding is complete (Figure 1E). In the far-UV CD, the spectra of wild-type StAR and mutant StAR had minima at 208 and 222 nm, typical of an α-helical conformation. The calculated (*45, 46*) secondary structural characteristics of both the

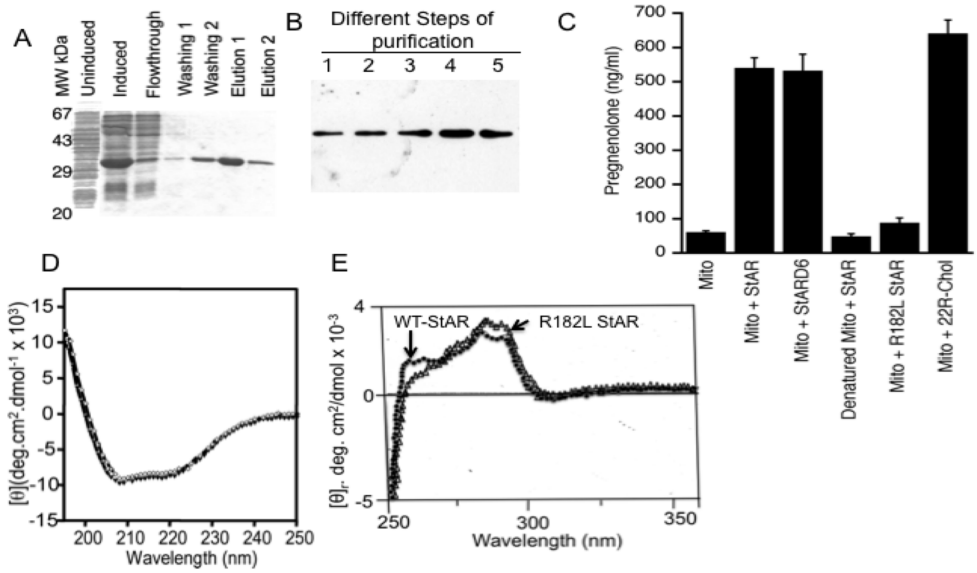

FIGURE 1: Characterization of wild-type and mutant StAR proteins. N-62 StAR wild type and mutant StAR were purified from bacterial cytosol, and activity was determined. Panel A: Typical elution nature of one of the StAR proteins used in these experiments. Panel B: Western blot of eluted fractions, including the major peak, probed with N-62 StAR antiserum. Panel C: Biological activity as measured by accumulated pregnenolone synthesis of the purified proteins after incubating with the isolated pig adrenal mitochondria at 37 °C. Panel D: Far-UV (195−250 nm) equilibrium circular dichroism (CD) spectra of wild-type StAR (---), mutant (○), and StARD6 (♦). Panel E: Near-UV CD spectrum at 250−360 nm of wild-type (●) and mutant R182LStAR (△) proteins at a concentration of 3.0 mg/mL. In panel C, data are mean ± SEM from three or four independent experiments, each performed in triplicate.

Table 1: Helical Content Comparison of the Wild-Type and Mutant StAR Protein and Its Comparison with the Crystal Structure

construct	helix (%)	sheet (%)	turn (%)	coil (%)
wild type	22.8	25.9	21.2	29.7
mutant (R182L)	22.5	26.8	20.9	29.3
StARD3[a]	26.7	37.4		
StARD4[b]	24.6	42.2		

[a] Taken from crystal structure (*18*). [b] Taken from crystal structure (*19*).

purified forms were very similar (Table 1) and closely match the helical content derived from the crystal structure (*18*). Thus, it is reasonable to assume that the purification procedure of these proteins was optimal.

Characterization of the Tryptophan Environment. Wild-type and mutant StAR binds with cholesterol almost at the same efficiency (*23, 32*), but bioactivity or secondary structural measurement or thermodynamic measurement failed to explain the reason for the inability of the mutant form to transport cholesterol. Thus, these experiments suggest that the microenvironment of wild-type StAR and mutant StAR may be different. Tryptophan (Trp) fluorescence is a powerful tool for studying protein structure function, due primarily to different rates of electron transfer from the excited indole ring of the Trp molecule to one of the two nearest backbone amides. This dependence on protein environment arises mainly from the average local electric potential difference between the Trp ring and acceptor amide and from the amplitude of potential difference fluctuation caused by protein and solvent motions. Thus the intrinsic fluorescence of Trp residues provides a sensitive means to probe the tryptophan microenvironment of a protein. We determined the microenvironment of the Trp residues by fluorescence spectroscopy using an equal amount of both the wild-type and mutant StAR. To determine the contribution of tyrosine residue in the protein, we also excited at 280 nm which contributes the fluorescence of both Trp and

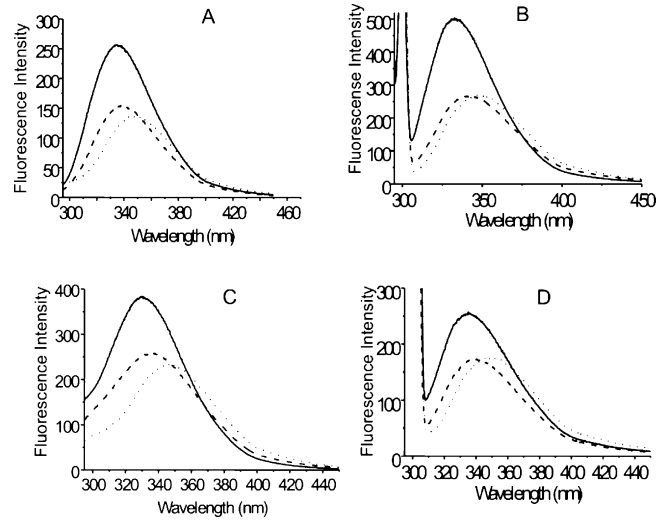

FIGURE 2: Trp fluorescence spectroscopy. Wild-type (N-62 StAR) (A and B) and mutant (R182L) StAR (C and D) at pH 7.5 were incubated with 0 (—), 2 (---), and 8 (•••) M urea and excited at 280 nm (A and C) and 295 nm (B and D). The spectra were plotted after subtraction of the buffer blank.

Tyr. The wild-type and mutant StAR proteins have four Trp residues distributed through out the sequence at positions 96, 147, 241, and 250. At an excitation of 280 nm, wild-type StAR had a Trp emission maximum at 337.5 ± 0.3 nm (Figure 2A), but mutant StAR had a fluorescence maximum of 331 nm (Figure 2C), suggesting that mutant StAR is more shielded than wild-type StAR. Gradual addition of a denaturant, such as urea, showed a difference in fluorescence intensity maxima. The wild-type protein intensity maxima at 0, 2, and 8 M urea were 337, 340, and 350 nm, respectively (Figure 2A), whereas mutant StAR showed intensity maxima at 331, 335, and 343 nm, respectively (Figure 2C). Similar results were observed when excited at 295 nm for wild-type (Figure 2B) and mutant StAR (Figure 2D). Thus, the Trp

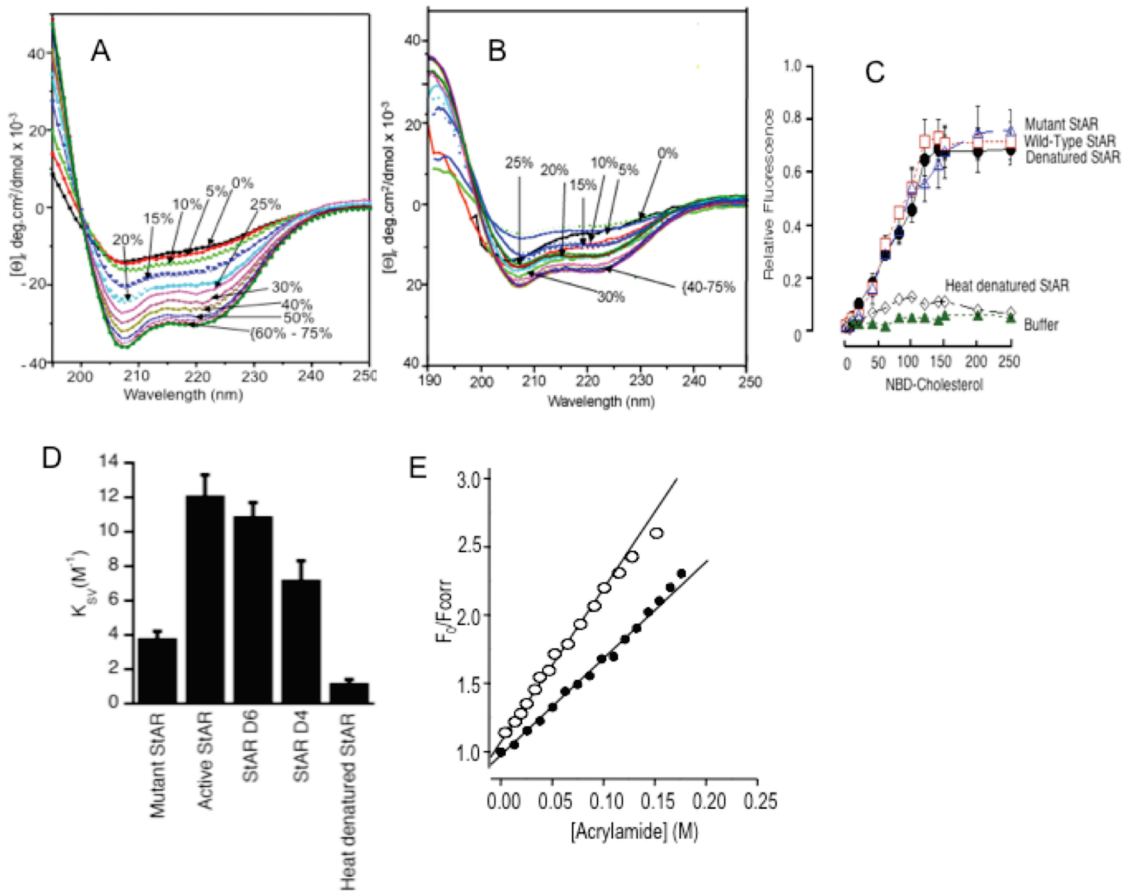

FIGURE 3: Relative stabilization of wild-type and mutant StAR by TFE. Panel A and B: Far-UV CD spectra of wild-type and mutant StAR with increasing concentrations of TFE. The spectra in panels A (wild type) and B (mutant) are labeled with the percentage of TFE. The α-helical minima of wild-type StAR (A) is increased more than mutant (B). Panel C:, Binding of wild type, mutant protein, denatured protein, and heat-denatured StAR and protein with increasing concentration of NBD-cholesterol. The relative intensity of the fluorescence intensity maximum at 560 nm was plotted against NBD cholesterol concentration. In all panels, data are mean SEM from three or four independent experiments, each performed in triplicate. Panel D: Acrylamide quenching of Trp fluorescence (K_{SV}) for the wild-type and mutant proteins. Panel E: Binding of acrylamide to wild-type (○) and mutant StAR (■), as measured by F_0/F_{cor}. In panels C and D, data are mean ± SEM from four independent experiments, each performed in triplicate.

residues in mutant StAR are more shielded than the wild-type protein.

TFE stabilizes the α-helical conformation by acting within the context of a preexisting helix−coil equilibrium (*47*). This preferential interaction with the folded state helps in shifting the equilibrium toward a more structured conformation (*48*) by reinforcing hydrogen bonds between carbonyl and amide −NH groups by the removal of water molecules in the proximity of solutes (*49*). The addition of increasing concentrations of TFE from 5% to 75% increased the secondary structure as evidenced with the increase in intensity minima at 208 and 222 nm, typical of an α-helical conformation (Figure 3A). The intensity of the minima increased up to 60% TFE at 208 and 222 nm for wild-type StAR. This suggests a significant increase in α-helical conformation of wild-type StAR. Under similar conditions, mutant StAR increased its α-helical content up to 30% of TFE (Figure 3B). The mutant StAR protein in this experiment is a replacement of the polar amino acid arginine with apolar leucine. The ability of TFE to induce an α-helical conformation is reduced in mutant StAR, likely owing to the reduced hydrogen-bonding capacity of mutant StAR. The stability of the protein strongly depends on the protein environment (*50*). The pregnenolone synthesizing capacity of wild-type StAR is 7−9-fold higher than mutant StAR; thus we sought to determine whether wild-type and mutant StAR could bind cholesterol equivalently. Wild-type StAR binding of authentic [^{14}C]cholesterol and the somewhat larger fluorescent compound NBD-cholesterol is equivalent (*23*); hence we used assays with NBD-cholesterol. As the size of the two proteins is the same, we used the same amount of protein throughout the experiment; thus the relative change in fluorescence should be proportional to the binding of NBD-cholesterol. The binding assays yielded sigmoidal curves, as expected (*36*), showing that wild-type or mutant StAR or the denatured protein bound cholesterol equivalently (Figure 3C). As wild-type StAR binds cholesterol with nearly 1:1 stoichiometry (*18*), it would appear that binding of cholesterol is not associated with the discharging of cholesterol (*32*). The denatured protein is the same as wild-type StAR, which was solubilized with 8 M urea during purification from *E. coli* and refolded by removal of urea through gradual dialysis, as described (*27*). On the other hand, the denaturation of wild-type StAR by incubation in a boiling water bath (*7*) did not bind with NBD-cholesterol.

To further investigate the difference in microenvironment between these two proteins, we measured acrylamide quenching of Trp residues. Acrylamide is an electron-deficient compound that deactivates the excited fluorophores by collisional quenching (i.e., electrons are transferred from the

excited indole group to acrylamide). This quenching effect allows one to detect minor structural differences in protein molecules, since proteins with greater Trp accessibility and higher acrylamide binding undergo a greater decrease in fluorescence intensity. K_{SV}, which provides an index of quencher accessibility, was calculated for both wild-type StAR and mutant StAR based on the fluorescence intensity of each. For reference we employed the model Trp compound *N*-acetyl-L-tryptophanamide (NATA), which has a completely open chain conformation with a K_{SV} value of 16.5 ± 0.3 M^{-} (*1*). At an excitation of 295 nm, the K_{SV} of wild-type StAR (*32*) was 12.0 ± 0.2 M^{-1} and 11.2 ± 0.5 M^{-1} for StARD6, but mutant StAR was 4 ± 0.2 M^{-1} (Figure 3D). The addition of NaCl did not alter the K_{SV} value of the StAR proteins, showing that the enhanced acrylamide quenching was due to structural relaxation of the protein. These results demonstrate that wild-type StAR has a more open conformation than mutant StAR.

To determine the relative degree of flexibility between wild-type and mutant StAR, we measured the unquenched to quenched fluorescence (F_0/F_{corr}) of each protein in response to increasing acrylamide concentration. The higher (F_0/F_{corr}) values indicated higher binding efficiency due to the flexibility of the protein conformation (*51*). At 50 mM acrylamide, mutant StAR had a F_0/F_{corr} value of 1.1 but wild-type StAR had a value of 1.6. At a concentration of 100 mM, these values increased to 1.5 for mutant StAR and 2.3 for wild-type StAR (Figure 3E). At an even higher acrylamide concentration of 200 mM, the value for mutant StAR was 2.2; however, that for wild-type StAR was greater than 3.0. These higher F_0/F_{corr} values for wild-type StAR suggest that this form of the protein has a greater binding capacity for acrylamide than the mutant. The increased acrylamide binding capacity suggests higher accessibility of acrylamide with the wild-type protein than the mutant StAR protein. This is possibly due to the accessibility with the internal and surface-exposed Trp residues of the protein (*52*).

Protein Flexibility. The above experiments suggest that the hydrophobic core of wild-type StAR may be different from mutant StAR. To investigate this possibility, the proteins were probed with the fluorescent probe ANS. ANS has been extensively used to investigate protein hydrophobicity and conformational changes (*53*). When ANS is protected from aqueous quenching and therefore in a more hydrophobic environment, the emission intensity increases and the maximum shifts to a shorter wavelength. This so-called "blue shift" can be used as an index of the compactness or the flexibility of the folded protein. ANS binds to accessible hydrophobic areas and induces a conformational change in the protein such that the ANS molecule is in a more hydrophobic environment (*53*). Therefore, ANS binds very strongly to proteins in a molten globule conformation due to the flexible tertiary structure (*51*); however, it does not bind efficiently to denatured proteins or proteins with well-packed structures. The ANS molecule has two broad overlapping absorption bands, and upon excitation at 357 nm in an aqueous medium, emission intensity maxima appear at ~525 nm with a very low quantum yield. In the presence of either wild-type or mutant StAR, the fluorescence emission of ANS increased with a blue shift of the fluorescence emission maxima to 470 nm (Figure 4A,B). For wild-type StAR, addition of an increasing concentration of ANS to a fixed concentration of wild-type StAR (20 pmol) (Figure 4A) increased fluorescence, until it reached a plateau, suggesting that the ANS is bound to the surface of the protein. On the contrary, the intensity maxima of mutant StAR (Figure 4B) did not increase proportionately. In the absence of ANS, the intensity maxima was 125 au, and in the presence of 5 μM ANS the intensity maxima increased to 175 au, suggesting that mutant StAR did not bind ANS as strongly as wild-type StAR. A comparison of the binding efficiency of these two proteins revealed that, at any concentration of ANS, the emission intensity is 2.5 times greater for wild-type StAR than for mutant StAR, indicating that these two proteins differ with respect to their flexibility as wild-type can accommodate ANS and adapt a conformation that allows ANS to be in a more hydrophobic environment (Figure 4A,B). These results suggest that wild-type StAR has a more molten globule-like conformation than mutant StAR. The results presented in Figure 4A,B show that addition of ANS to wild-type StAR, but not mutant StAR, yielded very high intensities. To determine the stoichiometry of StAR binding with the ANS molecule, we determined the binding ratio by a Job's plot. A Job's plot allows one to determine the binding ratio by a continuous variation of the components (*54*). In the continuous variation method the total concentration of protein and ligand is fixed; however, the fraction of each is varied. From the maximum in the plot the binding stoichiometry can be determined. For example, if the maximum occurs at a mole fraction of 0.5, this would indicate 1:1 binding stoichiometry. In the current experiment the protein-to-ANS binding ratio for wild-type StAR was 1:1.2 (Figure 4C), and that for mutant StAR was 1:0.7 (Figure 4D).

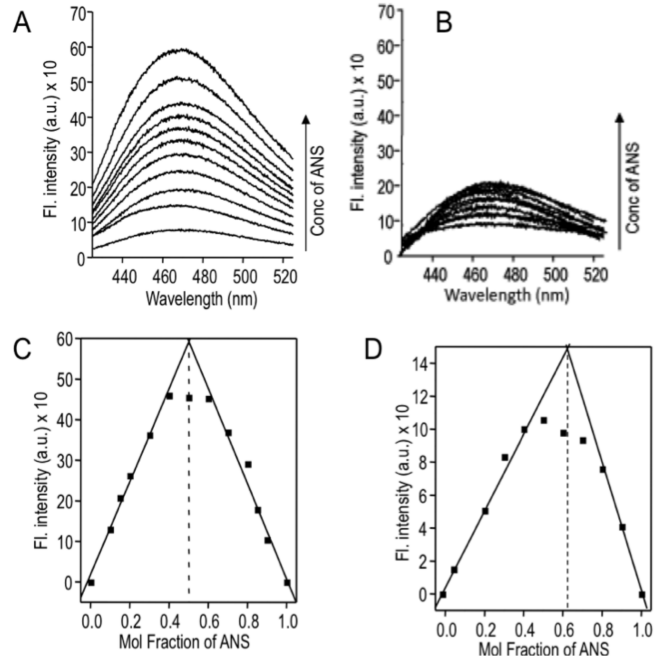

FIGURE 4: ANS binding analysis of wild-type and mutant StAR. Panels A and B: Emission spectra of increasing ANS concentration in the presence of a fixed amount of wild-type (A) and mutant StAR (B). Panel C and D: Stoichiometry of ANS binding to wild-type (C) and mutant StAR (D) as shown by a Job's plot. This Job's plot was generated from intensities at 470 nm and was obtained by fitting data points, in the range of 0−1.0 mole fractions of ANS, to a linear equation by the least-squares method (solid lines).

As ANS does not bind effectively to either fully denatured or the well-packed tightly folded protein (*51*), so the

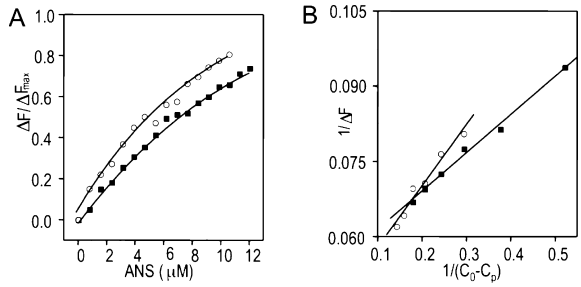

FIGURE 5: Effect of ANS binding with wild-type and mutant StAR. Panel A: The relative ratio of acrylamide binding ($\Delta F/\Delta F_{max}$) for wild-type (○) and mutant StAR (■) in response to increasing concentrations of ANS. Panel B: The apparent binding constant was determined by plotting the reciprocal of the difference in intensity (ΔF) against the reciprocal of the difference in the initial (C_0) and final concentration (C_p) of ANS.

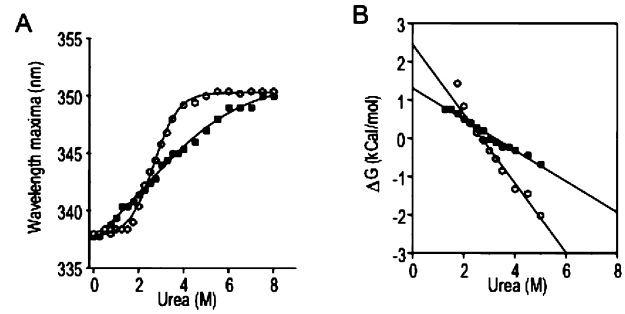

FIGURE 6: Urea denaturation of wild-type and mutant StAR. Panel A: Equivalent amounts of wild-type (○) and mutant (R182L) (■) StAR were equilibrated overnight with the indicated concentrations of urea, and the fluorescence emission maxima were measured after excitation at 295 nm. Panel B: Measurement of the free energy change (ΔG) and surface area (m) associated with urea denaturation of wild-type (○) and mutant (■) StAR, showing variations in ΔG as a function of urea concentration at an excitation of 295 nm.

reduction in binding of mutant StAR indicates it is less flexible in comparison to wild-type StAR. To quantify the flexible conformation (molten globule character) of each protein preparation, we titrated ANS with wild-type StAR and estimated binding by determining the difference in fluorescence at each concentration of ANS with respect to the fluorescence maxima ($\Delta F/\Delta F_{max}$). As shown in Figure 5A, the binding of wild-type StAR was greater than that of mutant StAR at all concentrations of ANS tested. We next determined the apparent binding of the StAR proteins with ANS. The apparent binding constant (K_{app}) was 8.1×10^5 M^{-1} for wild-type StAR but 3.75×10^5 M^{-1} for mutant StAR (double reciprocal plots are shown in Figure 5B). Changing the ionic environment of wild-type StAR from NaH_2PO_4 buffer to NaOAc buffer at pH 7.4 had no effect on the apparent binding, suggesting that the ionic environment has little direct effect on the conformation of the protein. High ionic strength may open the core of the protein, causing partial denaturation and replacement of the ANS; however, adding 10 mM to 1.0 M NaF to 5 μM StAR in phosphate buffer at pH 7.4 had no visible effect on the emission spectrum (data not shown).

StAR Stability. As a measure of protein stability, the difference in free energy of unfolding was determined in the presence of urea. From the unfolding curve, we measured the free energy of unfolding (ΔG) and determined the solvent denaturant value (m-value) by linear extrapolation. ΔG reflects the stability of a protein, and the m-value measures the rate of change of ΔG as a function of chaotrope concentration (*55*). A lower ΔG (unfolding) indicates that a protein is less stable, and a higher value indicates greater stability. Denaturants destabilize the protein structure by interacting favorably with proteins in their unfolded state (*55*). The m-value is proportional to the new surface area of protein that is accessible upon unfolding (*55*). Monitoring the fluorescence emission maxima following excitation at 295 nm revealed that wild-type StAR displayed typical two-step unfolding kinetics in the presence of increasing concentrations of urea. The protein remained tightly folded in 1.75 M urea and became completely unfolded in 4.0 M urea, with a midpoint at 3 M urea (Figure 6A). At the higher urea concentration, the curves for wild-type and mutant StAR overlap, suggesting that the Trp residues were randomly distributed. In contrast to the coordinated unfolding of wild-type StAR, mutant StAR did not display any cooperative transition (Figure 6A). That is, the protein gradually melted as the urea concentration increased, suggesting that it was folded differently than wild-type StAR. ΔG for wild-type StAR was 2.5 kcal/mol with an m-value of -0.9 but ΔG of mutant StAR was 1.3 kcal/mol with an m-value of -0.4 (Figure 6B). As these data were obtained at an excitation of 295 nm, they mainly reflect the microenvironment of the Trp residues and not the overall conformational state of the protein.

Proteolytic Digestion and Mass Spectrometric Analysis of StAR Proteins. Differences in StAR binding with ANS and enhanced stabilization with TFE suggest that there may be differences in the overall organization of the wild-type StAR and mutant StAR proteins. To examine these possibilities, we performed limited proteolysis of wild-type and mutant StAR at pH 7.4. Trypsin catalyzes specific cleavage after lysine and arginine residues under mildly alkaline conditions (at or above pH 7.0). Proteolytic digestion can be used to examine clearly the conformation of a protein, since the proteolytic pattern depends on the accessibility of the cleavage sites to the protease. If the accessibility of the cleavage site varies with changes in conformation, then different proteolytic patterns will emerge. The arrow indicates the proteolysis protected band (Figure 7).

The proteolytic digestion of wild-type StAR showed the complete amino acid sequence, except the five amino acids from 189−193 (CAKRR). These five amino acids were not observed, because this short sequence, containing three cleavage sites, results in short peptides that are not retained on the UPLC trapping column. Digestion of wild-type StAR with trypsin for up to 30 min using 10 units of enzyme resulted in an 18 kDa protein band, which on longer incubation was proteolyzed completely (Figure 7A, lower band). Excision of the trypsin-protected band followed by analysis with mass spectrometry showed that the amino acids from 63 to 188 were protected while the rest of the protein was proteolyzed. However, under identical conditions, even after longer incubation for up to 60 min, mutant StAR was protected (Figure 7B). Analysis of the relatively less intense 13 kDa band showed a mixture of N-terminal and C-terminal amino acids. Further analysis of the band showed complete amino acid sequence coverage of the protein, suggesting that this band is a mixture of possibly two similarly sized protein sequences, which were not clearly distinguishable in the gel. The mass spectrometric results of the protease-resistant and protease-sensitive regions are shown in the form of a cartoon (Figure 7C). As shown the C-terminus of wild-type StAR

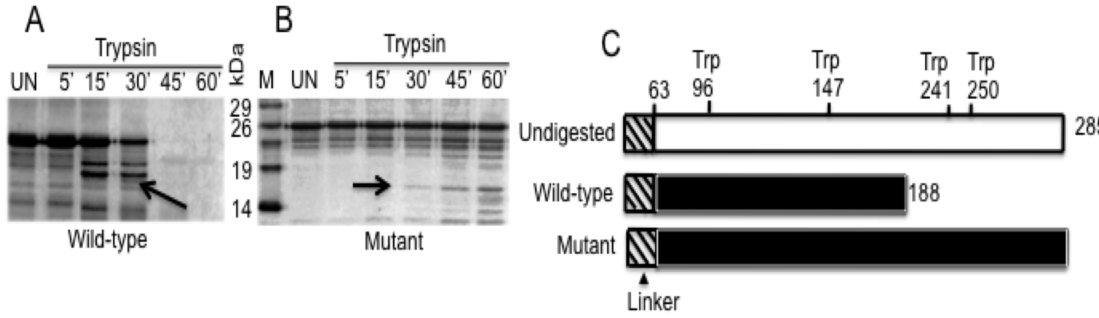

FIGURE 7: Proteolytic digestion of StAR. Panels A and B: Tryptic digestion of 5 μg of wild-type (A) and mutant StAR (B). Both of the proteins were digested at room temperature for a different period of time, electrophoresed on 20% SDS−PAGE, and stained with Coomassie blue. The trypsin-resistant bands, indicated by the arrowhead, and the undigested bands were excised from the gel and subjected to mass spectrometric analysis. Panel C: Summary of the identified protease-resistant amino acid region. The hatched region is the histidine linker. The dark region is the protected sequence.

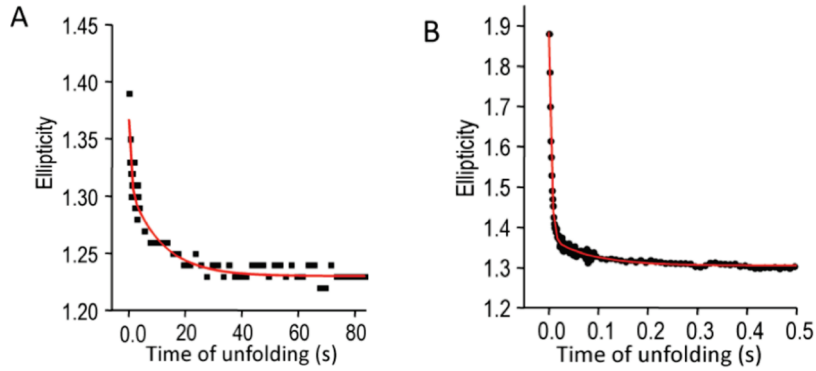

FIGURE 8: Folding and unfolding kinetics of wild-type and mutant StAR as determined by stopped-flow CD. The spectra of wild-type and mutant StAR are shown in panels A and B, respectively. For mutant StAR, a large fraction of the burst phase was recovered during the folding reaction.

remains flexible, allowing it to be in a transiently native-like state, molten globule conformation. This specific characteristic is missing with mutant StAR.

Real-Time Unfolding by Stopped-Flow Fluorescence. The unfolding experiments described above were carried out after incubating the proteins at room temperature overnight, and thus, they reflected gradual unfolding. To investigate the unfolding kinetics in real time, we used stopped-flow CD. Stopped flow is a device that can measure unfolding and refolding kinetics in real time. It requires rapid mixing experiments in which a protein in buffer is suddenly mixed with a high concentration of a chaotrope, such as urea or guanidine hydrochloride. The times required for conformational changes in the protein are then measured in milliseconds by circular dichroism and/or fluorescence emission (following excitation at 295 nm for Trp or at 280 nm). We performed the real time unfolding experiments by monitoring the CD signal at 222 nm. The results revealed that, for both wild-type StAR and mutant StAR, protein unfolding followed a unique opening after a burst phase (i.e., intermediate state of unfolding), which was not buried within the dead time. The proteins were unfolded when the urea concentration reached 5.0 M. No unfolding was observed at lower concentrations. Fitting the data with a biexponential decay equation revealed that both proteins had fast and slow unfolding rate constants, indicating biphasic unfolding. The times of unfolding were 16.3 s for StAR (Figure 8A) and 0.017 s for the mutant StAR (Figure 8B). The refolding could not be analyzed under the same conditions. The slower unfolding of wild-type StAR suggests that there is no rearrangement during unfolding and that the protein can maintain a parallel kinetic channel. Since the middle phase, which represents a transition to the native state, was not detectable, we cannot predict the much lower obligatory step (*56*).

DISCUSSION

In this study, we have demonstrated the internal differences between wild-type StAR and mutant StAR proteins. The wild-type StAR conformation has approximately twice as many ANS binding sites as mutant StAR. Similar findings have been reported for other proteins (*57*). Several lines of evidence (*58*) suggest that ANS binds to hydrophobic regions near planar aromatic rings that are in contact with hydrophobic regions, whereas the charged groups are in contact with water. The finding that the free energy (ΔG) for all the proteins is very close suggests that there is a difference in the internal hydrophobic groove of the wild-type and mutant proteins. The K_{app} of wild-type StAR is twice that of the mutant protein. It is likely that the groove in wild-type StAR is not globular (*18*), whereas the mutant StAR protein may adopt a more globular form, resulting in limited space and less flexibility.

The biochemical study only suggests that the Trp residues are randomly distributed, suggesting that the two Trp residues are more exposed than the others. It is likely that the organization of the wild-type StAR is more context dependent (*50*). StAR requires interaction with the outer mitochondrial membrane to adopt an open conformation (*30*). This conformational change is essential not for the binding of cholesterol but for the transfer of cholesterol into the mitochondria (*23, 30*). StAR docks for a short time on the OMM resident VDAC1 prior to its further

processing (*10*). Real-time assessments of wild-type and mutant StAR unfolding suggest that, for both forms of the protein, the fast phase is not associated with rapid collapse of the polypeptide chain and, therefore, it should be able to function as an intermediate state. Aromatic CD showed that both the wild-type and mutant StAR are folded. There is a small difference in ellipticity at 275 nm between these two proteins, and this is the position of tryptophan absorption. Thus, the core of each protein has a similar hydrophobic nature. Nevertheless, given the fact that activity is induced following unfolding, subtle differences may exist between the unfolding of the wild-type and the mutant forms of StAR (*8, 26*). Therefore, the faster unfolding of mutant StAR is not the sole reason for its inactivity, as we hypothesized earlier (*32*). Instead, the core of the protein may be folded differently than the outer part of the protein.

The broad unfolding of the burst-phase intermediate, the rapidity of its transition state, and the presence of a hydrophobic core in the intermediate are all typical characteristics of a molten globule state (*60*−*63*). Thus, the intermediate state of wild-type StAR is the same species as the molten globule state. The secondary structures formed in the molten globule state are native-like. The 2-fold difference in K_{app} values between wild-type StAR and mutant StAR suggests that the accessibility of ANS with the hydrophobic inner region differs between the two proteins. Further support for this difference is provided by the finding that the intensity of emission of wild-type StAR is 3-fold greater than mutant StAR and that a higher mole fraction of ANS was present in wild-type StAR. Moreover, TFE addition shifts toward a more structured folding by reinforcing the hydrogen bonding between carbonyl and amide −NH groups due to the removal of water molecules resulting in a more stable conformation (*49*). Because the OMM association property of StAR, the interaction between StAR and OMM is facilitated by the liberation of water molecules during StAR's transient stay at the OMM. Thus water molecules at the OMM play a significant role on the folding and interaction of StAR with the mitochondrial membrane. This is faciliatated only when the protein retains water molecules in its core. Addition of TFE modifies the membrane conformation similarly as it remains associated with the OMM by removing water between the core of StAR, resulting in increased α-helical conformation. Easy proteolysis of the wild-type StAR C-terminus confirmed that the C-helix, which is made by the carboxy terminus, keeps the folding in a pseudostable, native-like conformation (*20*). This flexibility of the C-helix (*21, 59*) allows wild-type StAR to hold and release cholesterol during its interaction with the OMM protein(s) (*10*) or at the time of release of cholesterol from the core to OMM. Taken together all of these facts, we can summarize that the differences in the hydrophobic core somehow affect the flexibility of the protein. The core of wild-type StAR is likely more nucleated than mutant StAR. In the nucleation−condensation protein folding model, the formation of a weak nucleus is associated with a compaction of the polypeptide chain, such that the tertiary and secondary structures are formed at the same time (*60*). However, the formation of a relatively small folding nucleus is not the only rate-determining step since a significant fraction of the overall structure should be in the correct conformation to link residues in the nucleus, so that it is able to come together. This type of behavior implies that folding is driven by the formation of a weak nucleus, where most of the polypeptide chain is involved in stabilizing the transition state of the protein. In the case of wild-type StAR, the flexible outer membrane likely acts to shield the weak nucleus, resulting in a 2-fold greater apparent binding. Thus, a loose hydrophobic core might be necessary to impart flexibility to StAR and to give it the ability to bind and release cholesterol.

ACKNOWLEDGMENT

H.S.B. is thankful to Dr. Michael Baldwin of The Buck Institute for Age Research for critical reading of the manuscript. H.S.B. is also thankful to Brian Adams for critically reading the manuscript. The authors D.D. and M.B. were postdoctoral fellows with H.S.B.

REFERENCES

1. Dobson, C. M., and Karplus, M. (1999) Understanding protein folding via free-energy surfaces from theory and experiment. *Trends Biochem. Sci. 25*, 331–339.
2. Sohl, J. L., Jaswal, S. S., and Agard, D. A. (1998) Unfolded conformations of α-lytic protease are more stable than its native state. *Nature 395*, 817–819.
3. Bilsel, O., and Matthews, C. R. (2000) Barriers in protein folding. *Adv. Protein Chem. 53*, 153–207.
4. Alm, E., and Baker, D. (1999) Prediction of protein-folding mechanisms from free energy landscapes derived from native structures. *Proc. Natl. Acad. Sci. U.S.A. 96*, 11305–11310.
5. Friel, C. T., Beddard, G. S., and Radford, S. E. (2004) Switching two-state to three-state kinetics in the helical protein Im9 via the optimisation of stabilizing nonnative interactions by design. *J. Mol. Biol. 342*, 293–305.
6. Stocco, D. M., and Clark, B. J. (1996) Regulation of the acute production of steroids in steroidogenic cells. *Endocr. Rev. 17*, 221–244.
7. Bose, H. S., Lingappa, V. R., and Miller, W. L. (2002) Rapid regulation of steroidogenesis by mitochondrial protein import. *Nature 417*, 87–91.
8. Bose, H. S., Sugawara, T., Strauss, J. F., III, and Miller, W. L. (1996) The pathophysiology and genetics of congenital lipoid adrenal hyperplasia. *N. Engl. J. Med. 335*, 1870–1878.
9. Arakane, F., Kallen, C. B., Watari, H., Foster, J. A., Sepuri, N. B. V., Pain, D., Stayrook, S. E., Lewis, M., Gerton, G. L., and Strauss, J. F., III (1998) The mechanism of action of steroidogenic acute regulatory protein (StAR): StAR acts on the outside of mitochondria to stimulate steroidogenesis. *J. Biol. Chem. 273*, 16339–16345.
10. Bose, M., Whittal, R. M., Miller, W. L., and Bose, H. S. (2008) Steroidogenic activity of StAR requires contact with mitochondrial VDAC1 and phosphate carrier protein. *J. Biol. Chem. 283*, 8837–8845.
11. Alpy, F., and Tomasetto, C. (2005) Give lipids a START: the StAR-related lipid transfer (START) domain in mammals. *J. Cell Sci. 118*, 2791–2801.
12. Soccio, R. E., and Breslow, J. L. (2003) StAR-related lipid transfer (START) proteins: mediators of intracellular lipid metabolism. *J. Biol. Chem. 278*, 22183–22186.
13. Iyer, L. M., Koonin, E. V., and Aravind, L. (2001) Adaptations of the helix-grip fold for ligand binding and catalysis in the START domain superfamily. *Proteins: Struct., Funct., Genet. 43*, 134–144.
14. de Brouwer, A., Bouma, B., van Tiel, C., Heerma, W., Brouwers, J., Bevers, L., Westerman, J., Roelofsen, B., and Wirtz, K. (2001) The binding of phosphatidylcholine to the phosphatidylcholine transfer protein: affinity and role in folding. *Chem. Phys. Lipids 112*, 109–119.
15. Harikrishna, J. A., Black, S. M., Szklarz, G. D., and Miller, W. L. (1993) Construction and function of fusion enzymes of the human cytochrome P450scc system. *DNA Cell Biol. 12*, 371–379.

16. Bose, H. S., Whittal, R. M., Huang, M. C., Baldwin, M. A., and Miller, W. L. (2000) N-218 MLN64, a protein with StAR-like steroidogenic activity is folded and cleaved similarly to StAR. *Biochemistry 39*, 11722–11731.
17. Soccio, R. E., Adams, R. M., Romanowski, M. J., Sehayek, E., Burley, S. K., and Breslow, J. L. (2002) The cholesterol-regulated StarD4 gene encodes a StAR-related lipid transfer protein with two closely related homologues, StarD5 and StarD6. *Proc. Natl. Acad. Sci. U.S.A. 99*, 6943–6948.
18. Tsujishita, Y., and Hurley, J. H. (2000) Structure and lipid transport mechanism of a StAR-related domain. *Nat. Struct. Biol. 7*, 408–414.
19. Romanowski, M. J., Soccio, R. E., Breslow, J. L., and Burley, S. K. (2002) Crystal structure of the *Mus musculus* cholesterol-regulated START protein 4 (StarD4) containing a StAR-related lipid transfer domain. *Proc. Natl. Acad. Sci. U.S.A. 99*, 6949–6954.
20. Roderick, S. L., Chan, W. W., Agate, D. S., Olsen, L. R., Vetting, M. W., Rajashankar, K. R., and Cohen, D. E. (2002) Structure of human phosphatidylcholine transfer protein in complex with its ligand. *Nat. Struct. Biol. 9*, 507–511.
21. Baker, B.-Y., Yaworsky, D. C., and Miller, W. L. (2005) A pH-dependent moltenglobule transition is required for activity of the steroidogenic acute regulatory protein, StAR. *J. Biol. Chem. 280*, 41743–41750.
22. Roostaee, A., Barbar, E., Lehoux, J. G., and Lavigne, P. (2008) Cholesterol binding is a prerequisite for the activity of the steroidogenic acute regulatory protein (StAR). *Biochem. J. 412*, 553–562.
23. Baker, B.-Y., Epand, R. F., Epand, R. M., and Miller, W. L. (2007) Cholesterol binding does not predict activity of the steroidogenic acute regulatory protein. *J. Biol. Chem. 282*, 10123–10132.
24. Liu, J., Rone, M. B., and Papadopoulos, V. (2006) Protein-protein interactions mediate mitochondrial cholesterol transport and steroid biosynthesis. *J. Biol. Chem. 281*, 38879–38893.
25. Arakane, F., King, S. R., Du, Y., Kallen, C. B., Walsh, L. P., Watari, H., Stocco, D. M., and Strauss, J. F., III (1997) Phosphorylation of steroidogenic acute regulatory protein (StAR) modulates its steroidogenic activity. *J. Biol. Chem. 272*, 32656–32662.
26. Christinsen, K., Bose, H. S., Harris, F. M., Miller, W. L., and Bell, J. D. (2001) Binding of StAR to synthetic membranes suggests an active molten globule. *J. Biol. Chem. 276*, 17044–17051.
27. Bose, H. S., Baldwin, M. A., and Miller, W. L. (1998) Incorrect folding of steroidogenic acute regulatory protein (StAR) in congenital lipoid adrenal hyperplasia. *Biochemistry 37*, 9768–9775.
28. Bose, M., Whittal, R. M., Gairola, C. G., and Bose, H. S. (2008) Cigarette smoke decreases mitochondria porin expression and steroidogenesis. *Toxicol. Appl. Pharmacol. 227*, 284–290.
29. Bose, M., Debnath, D., Chen, Y., and Bose, H. S. (2007) Folding, activity and import of steroidogenic acute regulatory protein (StAR) into mitochondria changed by nicotine exposure. *J. Mol. Endocrinol. 39*, 67–79.
30. Bose, H. S., Whittal, R. M., Baldwin, M. A., and Miller, W. L. (1999) The active form of the steroidogenic acute regulatory protein, StAR, appears to be a molten globule. *Proc. Natl. Acad. Sci. U.S.A. 96*, 7250–7255.
31. Wu, Y., Vadrevu, R., Kathuria, S., Yang, X., and Matthews, C. R. (2007) A tightly packed hydrophobic cluster directs the formation of an off-pathway submillisecond folding intermediate in the alpha subunit of tryptophan synthase, a TIM barrel protein. *J. Mol. Biol. 366*, 1624–1628.
32. Bose, H. S., Whittal, R. M., Ran, Y., Bose, M., Baker, B. Y., and Miller, W. L. (2008) StAR-like activity and molten globule behavior of StARD6, a male germ-line protein. *Biochemistry 47*, 2277–2288.
33. Gill, S. C., and von Hippel, P. H. (1989) Calculation of protein extinction coefficients from amino acid sequence data. *Anal. Biochem. 182*, 319–326.
34. Eftink, M. R., and Ghiron, C. A. (1981) Fluorescence quenching studies with proteins. *Anal. Biochem. 114*, 199–227.
35. Eftink, M. R. (1991) Fluorescence techniques for studying protein structure. *Methods Biochem. Anal. 35*, 127–205.
36. Petrescu, A. D., Gallegos, A. M., Okamura, Y., Strauss, J. F., III, and Schroeder, F. (2001) Steroidogenic acute regulatory protein binds cholesterol and modulates mitochondrial membrane sterol domain dynamics. *J. Biol. Chem. 276*, 36970–36982.
37. Yaworsky, D. C., Baker, B. Y., Bose, H. S., Best, K. B., Jensen, L. B., Bell, J. D., Baldwin, M. A., and Miller, W. L. (2005) pH-dependent Interactions of the carboxyl-terminal helix of steroidogenic acute regulatory protein with synthetic membranes. *J. Biol. Chem. 280*, 2045–2054.
38. Ali, V., Kulkarni, P. K., Ahmad, A., Madhusudan, K. P., and Bhakuni, V. (1999) 8-anilino-1-napthalenesulfonic acid (ANS) induces folding of acid unfolded cytochrome *c* to molten globule state as a result of electronic interactions. *Biochemistry 39*, 13635–13642.
39. Wang, J. L., and Edelman, G. D. (1971) Fluorescent pProbes for conformational states of protein. *J. Biol. Chem. 246*, 1185–1191.
40. Rosenfeld, J., Capdeville, J., Guillemot, J. C., and Ferrara, P. (1992) In-gel digestion of proteins for internal sequence analysis after one- or two-dimensional electrophoresis. *Anal. Biochem. 203*, 173–179.
41. Enoki, S., Maki, K., Inobe, T., Takahashi, K., Kiyoto, K., Oroguchi, T., Nakatani, H., Tomoyori, K., and Kuwajima, K. (2006) The equilibrium unfolding observed at pH 4 and its relationship with the kinetic folding in green fluorescent protein. *J. Mol. Biol. 361*, 969–982.
42. Pace, C. N. (1986) Determination and analysis of urea and guanidine hydrochloride denaturation curves. *Methods Enzymol. 131*, 266–280.
43. Bose, H. S., Baldwin, M. A., and Miller, W. L. (2000) Evidence that StAR and MLN64 act on the outer mitochondrial membrane as molten globules. *Endocr. Res. 26*, 629–637.
44. Fasman, G. D., Ed. (1996) *Circular dichroism and the conformational analysis of biomolecules*, Plenum Press, New York.
45. Sreerama, N., and Woody, R. W. (2004) Computation and alalysis of protein circular dichroism spectra. *Methods Enzymol. 383*, 318 Ch. 13.
46. Sreerama, N., and Woody, R. W. (2000) Estimation of protein secondary structure from CD soectra: Comparison of CONTIN, SELCON and CDSSTR methods with an expanded reference set. *Anal. Biochem. 282*, 252–260.
47. Del-Vercchiop, P., Graziano, G., Granata, V., Barone, G., Mandrich, L., Rossi, W., and Manco, G. (2003) Effect of trifluoroethanol on the conformational stability of a hyperthermophilic esterase: a CD study. *Biophys. Chem. 104*, 407–415.
48. Jasanoff, A., and Fersht, A. R. (1994) Quantitative determination of helical propensities from trifluoroethanol titration curves. *Biochemistry 33*, 2129–2135.
49. Luo, P., and Baldwin, R. L. (1997) Mechanism of helix induction by trifluoroethanol a framework for extrapolating the helix-forming properties of peptides from trifluoroethanol/water mixtures back to water. *Biochemistry 36*, 8413–8421.
50. Takano, K., Scholtz, J. M., Sacchettin, J. C., and Pace, C. N. (2003) The contribution of polar group burial to protein stability is strongly context-dependent. *J. Biol. Chem. 278*, 31790–31795.
51. Cunningham, E. L., and Agard, D. A. (2003) Interdependent folding of the N- and C-terminal domains defines the cooperative folding of alpha-lytic protease. *Biochemistry 42*, 13212–13219.
52. Alston, R. W., Lasagna, M., Grimsley, G. R., Scholtz, J. M., Reinhart, G. D., and Pace, C. N. (2008) Tryptophan fluorescence reveals the presence of long-range interactions in the denatured state of ribonuclease sa. *Biophys. J. 94*, 2288–2296.
53. Semisotnov, G. V., Rodionova, N. A., Razgulyaev, O. I., Uversky, V. N., Gripas', A. F., and Gilmanshin, R. I. (1991) Study of the molten globule intermediate state in protein folding by a hydrophobic fluorescent probe. *Biopolymers 31*, 119–128.
54. Huang, C. Y. (1982) Determination of binding stoichiometry by the continuous variation method: The Job Plot. *Methods Enzymol. 87*, 525–529.
55. Wrabl, J., and Shortle, D. (1999) A model of the changes in denatured state structure underlying m value effects in staphyloccal nuclease. *Nat. Struct. Biol. 6*, 876–883.
56. Bai, Y. (2003) Hidden intermediates and levinthal paradox in the folding of small proteins. *Biochem. Biophys. Res. Commun. 305*, 785–788.
57. Shi, L., Palleros, D. R., and Fink, A. L. (1994) Protein conformational changes induced by 1,1′-bis(4-anilino-5-napthalinosulfonic acid): preferential binding to the molten globule of DnaK. *Biochemistry 33*, 7536–7546.
58. Masui, R., and Kuramitsu, S. (1998) Probing of DNA-binding sites of *Escherichia coli* RecA protein utilizing 1-anilinonapthalene-8-sulfonic acid. *Biochemistry 37*, 12133–12143.
59. Mathieu, A. P., Fleury, A., Duchame, L., Lavigme, P., and LeHoux, J. G. (2002) Insights into steroidogenic acute regulatory protein (StAR)-dependent cholesterol transfer in mitochondria: evidence from molecular modeling and structure-based thermodynamics supporting the existence of partially unfolded ststes of StAR. *J. Mol. Endocrinol. 29*, 327–345.

60. Fersht, A. R. (1999) A kinetically significant intermediate in the folding of barnase. *Proc. Natl. Acad. Sci. U.S.A. 97*, 14121−14126.
61. Kuwajima, K., Yamaya, H., and Sugai, S. (1996) The burst-phase intermediate in the refolding of β-lactoglobulin studied by stopped-flow circular dichroism and absorption spectroscopy. *J. Mol. Biol. 284*, 806–822.
62. Bhuyan, A. K., and Udgaonkar, J. B. (2001) Folding of horse cytochrome *c* in the reduced state. *J. Mol. Biol. 312*, 1135−1160.
63. Privalov, P. L. (1996) Intermediate states in protein folding. *J. Mol. Biol. 258*, 707–725.

BI801514E